IEEE Access
Multidisciplinary ⋮ Rapid Review ⋮ Open Access Journal

Received April 7, 2020, accepted April 17, 2020, date of publication May 6, 2020, date of current version May 22, 2020.

Digital Object Identifier 10.1109/ACCESS.2020.2992708

Adaptive Sliding Mode Back-Stepping Speed Control of Hydraulic Motor for Wave Energy Conversion Device

WEI ZHANG[1], SHIZHEN LI[2], (Member, IEEE), AND YANJUN LIU[2]
[1]School of Mechanical and Electrical Engineering, Shandong Jianzhu University, Jinan 250101, China
[2]Institute of Marine Science and Technology, Shandong University, Qingdao 266237, China

Corresponding author: Shizhen Li (lishizhen@sdu.edu.cn)

This work was supported in part by the National Key Research and Development Program of China under Grant 2016YFE0205700, in part by the National Natural Science Foundation of China under Grant51705288, in part by the Doctoral Fund Research Project of Shandong Jianzhu University under ProjectX18036Z, and in part by the Open Foundation of the State Key Laboratory of Fluid Power and Mechatronic Systems, China, under Grant GZKF-201805.

ABSTRACT In order to improve the stability of the wave power generation device, the mechanism of variable displacement control mechanism of hydraulic motor is proposed and the control strategy of motor speed is built. The detailed mathematical representation and dynamic characteristics of motor control are analyzed; the adaptive sliding mode control method and a back-stepping control strategy are designed for the proposed controller to overcome the influence of the parameter uncertainty in the nonlinear system. The adaptive law is designed by Lyapunov criterion to ensure the stability and convergence of the whole closed-loop system. In order to verify the feasibility of the proposed control strategy, a wave power generation land experimental platform is designed, the experimental platform is mainly consists of the test bench bracket, the hydraulic transmission system and the electric power processing system. Through comparative analysis with PID control method, the advantages of this control method are described and the speed of motor can be controlled accurately.

INDEX TERMS Wave power generation device, variable displacement control, motor speed, back-stepping control strategy, land experimental platform.

I. INTRODUCTION

With the rapid development of economy, the demand for energy is increasing but the traditional energy is short, the use of a large number of fossil raw materials has caused serious ecological environment problems, which have caused serious pollution and damage to the ecological environment. The massive use of conventional energy such as coal, oil and natural gas has led to excessive carbon dioxide emissions and ''greenhouse effect'', which have led to accelerated melting of glaciers in the north and south poles, abnormal climate change, and more and more frequent natural disasters, seriously threatening the sustainable development of human society [1]–[3]. These problems have become the focus of attention all over the world. In order to deal with resource depletion and ecological environment problems and solve the bottleneck problem of energy supply in social and economic development, the development of renewable energy has become urgent. The establishment of a clean and renewable energy and gradually replacement of the fossil energy structure has a bearing on human survival and future [4], [5].

There are huge reserves of renewable energy in the ocean, among which the total amount of wave energy available is large [6], [7]. Because of its relatively high energy density and relatively low acquisition difficulty, the development of wave energy power generation technology has been paid more and more attention in many countries [8], especially the research and development of wave energy power generation technology [9]. As wave power generation equipment is not only affected by waves, but also by the joint action of sea wind and current, it puts forward higher requirements for the structural design of wave power generation equipment and how the energy transfer system can maintain normal operation in the complex marine environment [10]. Countries

The associate editor coordinating the review of this manuscript and approving it for publication was Feng Wu.

around the world have further strengthened policy support and increased capital investment in wave power generation technology, and have obtained great results.

The point absorbing wave energy generating device uses the float to sway with the wave, and drives the mechanical transmission device or the hydraulic device to realize the energy conversion and finally output the electric energy [11], [12]. The problem of unstable energy conversion in power generation equipment is a key technical problem to be solved in wave energy utilization. In the existing energy conversion device, most of the energy conversion system (PTO) uses hydraulic technology, which has been proved that it has the unique advantages in the energy transmission process of the power generation device.

Because the hydraulic transmission system can use the accumulator to store the hydraulic energy to buffer the random impact of waves, and can improve the stability of electric energy output through the volume speed regulation of variable motor [13], the hydraulic energy transmission technology is used as the intermediate link of energy conversion, which is widely used in the existing marine energy generation devices, and many devices which use the hydraulic transmission system as the power generation of energy conversion have been verified in sea trial. Scholars at home and abroad have carried out a large number of researches on wave energy power generation devices with hydraulic energy transmission, analyzed the composition and working principle of hydraulic energy conversion system of different types of wave power generation devices [14], [15]. This paper expounds the energy conversion mechanism of hydraulic conversion system and built land experimental platform to further study of the proposed control strategies. In order to improve the stability of the hydraulic transmission system and ensure that the generator speed can be stable in a certain range, a nonlinear control strategy is designed to track the motor speed [13], [16].

In this paper, the optimal point absorption wave power generation device will be used. The first part introduces the working principle of the hydraulic transmission system; the second part establishes the mathematical model; the third part establishes the control strategy; the fourth part constructs the land experiment platform to verify the theoretical results; the fifth part draws the conclusion.

II. WORKING PRINCIPLE OF WAVE ENERGY POWER GENERATION DEVICE

A. POWER GRNERATION PRINCIPLE

Fig. 1 shows a new wave energy power generation device. The device is mainly composed of wave energy conversion system, energy transfer system, electric energy consumption system and control detection system. It is using the hydraulic transmission system as energy transmission to improve the stability of electric energy output. The wave energy collection system can convert the wave energy into mechanical energy of float. The movement of float can convert the mechanical energy to hydraulic energy, which travels through the hydraulic system and drives the motor to rotate, thus driving the generator to work and output power stably.

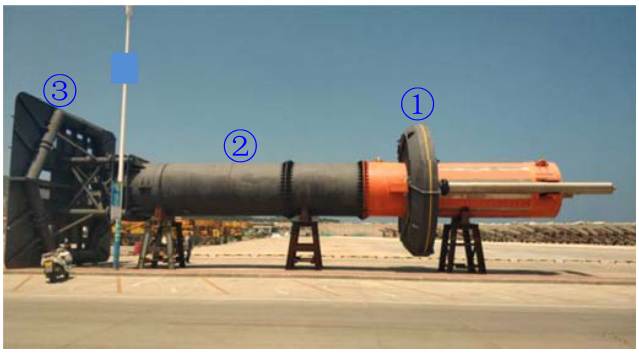

1. Float 2. Buoy 3. Damping plate

FIGURE 1. Wave energy power generation device.

B. PRINCIPLE OF HYDRAULIC TRANSMISSION SYSTEM

The specific working process of the hydraulic transmission system is shown in Fig. 2: the fluctuation of the wave causes the float to move up and down, and drives the hydraulic cylinder to work. The resulting high-pressure oil drives the hydraulic motor to rotate, drives the generator to generate electricity, and the hydraulic oil discharged by the hydraulic variable displacement motor is cooled by the oil tank before it is recycled by the hydraulic cylinder.

The hydraulic system has three different combinations of motor and generator, which are suitable for different wave conditions such as large wave, medium wave and wavelet, so as to ensure the reasonable distribution of obtained wave energy. This design can prevent the generator from burning when the wave energy is large. At the same time, it can assure the generator to be started when the wave energy is small, so as to ensure the working safety of the power generation equipment. In order to ensure the stability of output electric energy and overcome the influence of wave change on the hydraulic conversion, the variable motor speed control strategy is built when a set of motors and generators work. The research of motor speed control strategy is the focus of this paper.

The specific working process is when the wave is relatively large and wave energy is absorbed more, the large displacement variable motors will work to drive 55kW generators to work, and the high-pressure accumulator will start and store the excess energy in the accumulator; when the wave is smaller, and the energy collected by the power generation system is not enough to maintain the normal power generation of the system, the low-pressure accumulator will be started, and the pre-stored energy in the accumulator will be used for supplementary adjustment. At the same time, the small displacement hydraulic motor to drive the 18kW generator to work, and when it works in the medium wave condition, the 37 kW generator will work. In this way, it will improve the safety of power generation device and the efficiency of power output. By adjusting each group of variable motor, the speed

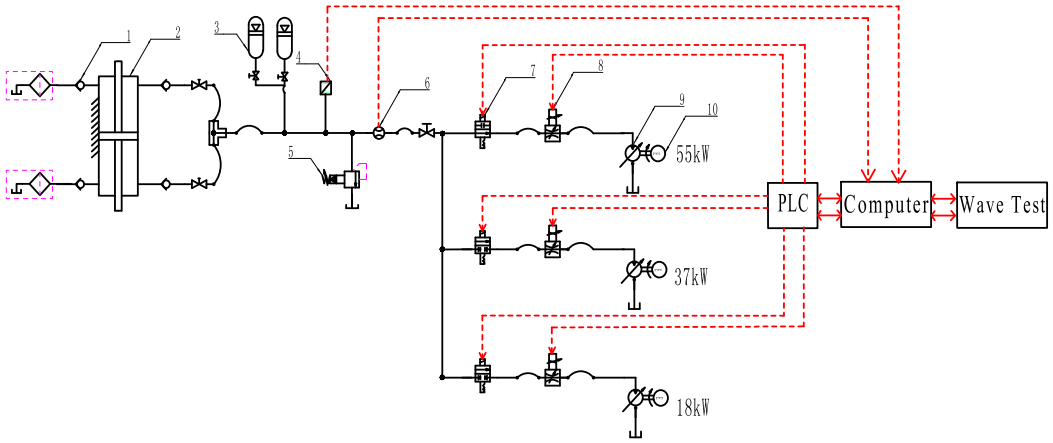

FIGURE 2. Working principle of hydraulic transmission system.

of the generator is kept in different stable range, and it is also convenient for the post-processing process such as rectifying, stabilizing and inverting of electric energy.

C. CONTROL PRINCIPLE OF HYDRAULIC MOTOR

When different wave conditions come, the flow of the system Q_i will change, it will affect the speed of the motor, and then affect the stability of the output electric energy. Therefore, in order to ensure the stability of hydraulic energy output, the motor displacement q_m can be controlled in real time according to the state of input flow, so as to ensure that the motor speed can be stable in a certain range.

The basic principle of hydraulic motor speed regulation is: when the input wave condition changes, the inclination angle of the swash plate is adjusted by the control strategy and the displacement of the hydraulic motor changes accordingly. The displacement change will cause the change of the motor output speed, so as to realize the adjustable electric energy output and improve the stability of the output electric energy. Because of the uncertainty of float motion and the uncertainty of load torque caused by the change of external load, the linear control strategy is difficult to meet the control requirements, and it can get a good control effect under the nonlinear control strategy. In this paper, the back-stepping method is applied to the speed control system of hydraulic motor and an adaptive sliding mode controller based on the back-stepping method is designed. The control schematic diagram of variable motor is shown in Fig. 3.

III. ESTABLISHMENT OF DYNAMIC MATHEMATICAL MODEL

The flow continuity equation of hydraulic motor is as follows:

$$Q_i = q_m\omega_m + \frac{U_p}{\beta_e}\cdot\dot{P}_h + C_mP_h \tag{1}$$

In formula: P_h is the input pressure to the hydraulic motor, Q_i is the input flow to hydraulic motor, q_m is the displacement of the hydraulic motor, ω_m is the hydraulic motor speed,

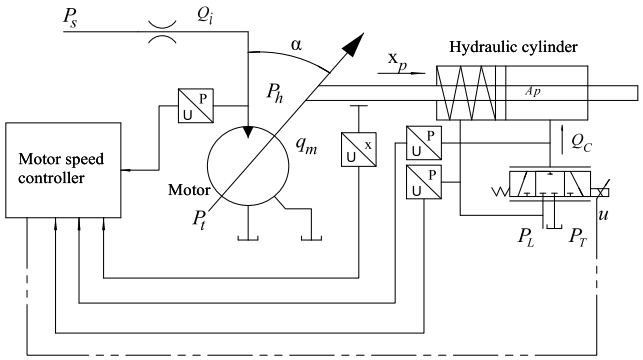

FIGURE 3. Control schematic diagram of variable motor.

C_m is the leakage coefficient. Up is the total volume of motor.

$$q_m = \frac{V_{\max}}{x_{\max}}x_p = k_px_p = \frac{V_{\max}}{\alpha_{\max}}\alpha \tag{2}$$

In style: q_m is the displacement of the hydraulic motor, $V_{\max}$ is the maximum displacement of the hydraulic motor, $x_{\max}$ is the maximum position of the hydraulic cylinder to control the swing angle of the hydraulic motor, k_p is the proportionality factor, x_p is the displacement of hydraulic cylinder, $\alpha_{\max}$ is the maximum swing angle of variable motor, α is real time swing angle for hydraulic motor, and we can get formula (3) by taking the derivative of formula (2):

$$\dot{q}_m = k_p\nu_p \tag{3}$$

In formula: ν_p is the hydraulic cylinder speed. The load moment balance equation of hydraulic motor is:

$$P_h\cdot q_m = J_m\cdot\dot{\omega}_m + B_m\cdot\omega_m + T_h \tag{4}$$

In formula: J_m is the coefficient of inertia, B_m is the viscous damping coefficient, T_h is the disturb load torque of motor. The force equation of the hydraulic cylinder is:

$$A_p\cdot p_l = m_p\cdot\dot{\nu}_p + B_p\cdot\nu_p + T_p \tag{5}$$

In formula: A_p is the effective area of hydraulic cylinder, p_l is the pressure at the outlet of servo valve, m_p is the effective piston mass. B_p is the piston viscous damping coefficient, T_p is the external disturbance torque of hydraulic cylinder. The relationship between simplified control input signal and servo valve displacement is:

$$x_p = k_q \cdot \mu \tag{6}$$

In formula: k_q is the proportionality factor of amplifier, μ is the input voltage. Then the flow equation of servo valve controlled hydraulic cylinder is:

$$k_q \cdot \mu\sqrt{p_s - p_l \mathrm{sgn}(x_p)} = A_p \cdot v_p + \frac{U_p}{\beta_e}\dot{p}_l + C_m \cdot p_l \tag{7}$$

In formula: p_s is the hydraulic pressure supplied by pressure source. p_l is the output pressure of hydraulic cylinder for servo valve, C_m is the leakage coefficient. sgn$(\cdot)$ is the sign function, its expression is:

$$\mathrm{sgn}(\cdot) = \begin{cases} 1, & \cdot \geq 0 \\ 0, & \cdot < 0 \end{cases} \tag{8}$$

By sorting out the above formula from (1) to (8), we can get the differential equations:

$$\begin{cases} \dot{\omega}_m = \dfrac{P_h}{J_m} \cdot k_p x_p - \dfrac{B_m}{J_m} \cdot \omega_m - \dfrac{T_h}{J_m} \\ \dot{v}_p = \dfrac{A_p}{m_p} \cdot p_l - \dfrac{B_p}{m_p} \cdot v_p - \dfrac{T_p}{m_p} \\ \dot{p}_l = k_q \cdot \mu\sqrt{p_s - p_l \mathrm{sgn}(x_p)} \cdot \dfrac{\beta_e}{U_p} - A_p \cdot v_p \cdot \dfrac{\beta_e}{U_p} - C_m \cdot p_l \cdot \dfrac{\beta_e}{U_p} \end{cases}$$

According to the differential equations, the speed of hydraulic motor is related to the input flow and external load of the hydraulic cylinder. The differential equations can be expressed as:

$$\begin{cases} \dot{\omega}_m = f_1 \cdot x_p - a_2 \cdot \omega_m - d_1 \\ \dot{v}_p = b_1 \cdot p_l - b_2 \cdot v_p - d_2 \\ \dot{p}_l = \mu \cdot g(p_l) - c_1 \cdot v_p - c_2 \cdot p_l \end{cases} \tag{9}$$

In formula:

$$\begin{cases} f_1 = \dfrac{P_h \cdot k_p}{J_m}; a_2 = \dfrac{B_m}{J_m}; d_1 = \dfrac{T_h}{J_m} \\ b_1 = \dfrac{A_p}{m_p}; b_2 = \dfrac{B_p}{m_p}; d_2 = \dfrac{T_p}{m_p} \\ g(p_l) = k_q \cdot \sqrt{p_s - p_l sgn(x_p)} \cdot \dfrac{\beta_e}{U_p}; c_1 = A_p \cdot \dfrac{\beta_e}{U_p}; \\ c_2 = C_m \cdot \dfrac{\beta_e}{U_p} \end{cases}$$

Define system state variables:

$$x = [x_1, x_2, x_3, x_4]^{\mathrm{T}} = \left[\omega_m, x_p, v_p, p_l\right]^{\mathrm{T}} \tag{10}$$

Then the state space expression of the system mathematical model is:

$$\begin{cases} \dot{x}_1 = f_1 \cdot x_2 - a_2 \cdot x_1 - d_1 \\ \dot{x}_2 = x_3 \\ \dot{x}_3 = b_1 \cdot x_4 - b_2 \cdot x_3 - d_2 \\ \dot{x}_4 = \mu \cdot g(x_4) - c_1 \cdot x_3 - c_2 \cdot x_4 \\ y = x_1 \end{cases} \tag{11}$$

IV. ESTABLISH THE CONTROL STRATEGY

A. THE DESIGN OF EXTERNAL OBSERVER

An external observer based on state variables x_1 is established to evaluate the unknown load disturbance. The dynamic observer is designed as:

$$\begin{cases} \hat{d} = \xi - Kx_1 \\ \dot{\xi} = K \cdot (f_1 x_2 - a_2 x_1) - \hat{d} \cdot K \end{cases} \tag{12}$$

In formula: $\hat{d}$ is the evaluation value of load and flow disturbance, ξ is the internal state of the load and flow observer, K is positive real number. Assumed that the load flow estimation error $\tilde{d} = d - \hat{d}$ of the disturbance observer is bounded, and converges to the sphere centered at the origin. Verify the convergence of the evaluation error $\tilde{d}$ as follows:

$$\begin{aligned} \dot{\tilde{d}} &= \dot{d} - \dot{\hat{d}} \\ &= \dot{d} - \dot{\xi} + K(f_1 x_2 - a_2 x_1 - d_1) \\ &= \dot{d} - K \cdot \tilde{d} \end{aligned} \tag{13}$$

Then, by defining V_d with Lyapunov function we can get:

$$\mathrm{V}_d = \frac{1}{2}\tilde{d}^2 \tag{14}$$

Deriving from the above formula:

$$\dot{V}_d = -K\tilde{d}^2 + \dot{d}\tilde{d} \tag{15}$$

Collate:

$$\begin{aligned} \dot{V}_d &\leq -(K - \varepsilon)\tilde{d}^2 + \frac{1}{4\varepsilon}\dot{d}^2 \\ &\leq -2(K - \varepsilon)V_d + \frac{1}{4\varepsilon}\mu^2 \end{aligned} \tag{16}$$

where ε is positive real number and satisfaction relation, $\varepsilon < K$.

Then the evaluation error $\tilde{d}$ of the load flow observer is bounded and converges to the circle with radius of $r_d = \frac{\mu}{2}\sqrt{\frac{1}{\varepsilon(K\frac{\beta}{V} - \varepsilon)}}$, if the state estimation of f_1 and a_2 are defined $\hat{f}_1$, $\hat{a}_2$ respectively, the error of state estimation value can be expressed:

$$\begin{cases} \tilde{f}_1 = f_1 - \hat{f}_1 \\ \tilde{a}_2 = a_2 - \hat{a}_2 \end{cases} \tag{17}$$

The dynamic differential equation expression of estimation error $\tilde{x}_{1\mathrm{p}}$ of state variable x_1 is:

$$\dot{\tilde{x}}_{1\mathrm{p}} = \dot{x}_1 - \dot{\hat{x}}_{1\mathrm{p}}$$

$$= \dot{x}_1 - (\hat{f}_1 x_2 - \hat{a}_2 x_1 - \hat{d}_1 + \Gamma \tilde{x}_{1p}) = \tilde{f}_1 x_2 - \tilde{a}_2 x_1 - \tilde{d}_1 - \Gamma \tilde{x}_{1p} \quad (18)$$

In formula: Γ is a positive feedback gain.

Defining Lyapunov function:

$$V_1 = \frac{1}{2} k_{11} \tilde{x}_{1p}^2 + \frac{1}{2} k_{12} \tilde{a}_2^2 + \frac{1}{2} k_{13} \tilde{d}_1^2 + \frac{1}{2} k_{14} \tilde{f}_1^2 \quad (19)$$

Differentiation of the above formula:

$$\begin{aligned} \dot{V}_1 &= k_{11} \tilde{x}_{1p} \cdot \dot{\tilde{x}}_{1p} + k_{12} \tilde{a}_2 \cdot \dot{\tilde{a}}_2 + k_{13} \tilde{d}_1 \cdot \dot{\tilde{d}}_1 \\ &= k_{14} \tilde{f}_1 \cdot \dot{\tilde{f}}_1 k_{11} \tilde{x}_{1p} \cdot (\tilde{f}_1 x_2 - \tilde{a}_2 x_1 - \tilde{d}_1 - \Gamma \tilde{x}_{1p}) \\ &\quad + k_{13} \tilde{d}_1 \cdot \dot{\tilde{d}}_1 + k_{14} \tilde{f}_1 \cdot \dot{\tilde{f}}_1 + k_{12} \tilde{a}_2 \cdot \dot{\tilde{a}}_2 \end{aligned} \quad (20)$$

Collate:

$$\begin{aligned} \dot{V}_1 &= \tilde{f}_1 (k_{11} \tilde{x}_{1p} \cdot x_2 + k_{14} \cdot \dot{\tilde{f}}_1) \\ &\quad + \tilde{a}_2 (k_{12} \cdot \dot{\tilde{a}}_2 - k_{11} \tilde{x}_{1p} \cdot x_1) \\ &\quad + \tilde{d}_1 (k_{13} \cdot \dot{\tilde{d}}_1 - k_{11} \tilde{x}_{1p}) - k_{11} \tilde{x}_{1p}^2 \cdot \Gamma \end{aligned} \quad (21)$$

In formula: $k_{11}, k_{12}, k_{13}, k_{14}$, are the positive constants.

B. THE DISPLACEMENT ADAPTIVE SOULATION OF THE HYDRAULIC CYLINDER CONTROLLING THE SWING ANGLE

If the expected value of hydraulic motor speed is defined as x_{1d}, the motor speed tracking error expression is:

$$z_1 = x_1 - x_{1d} \quad (22)$$

In order to eliminate the approximation error of the adaptive system, the integral sliding mode theory is used to compensate it. Define the integral sliding surface as s, the expression of integral sliding surface is designed:

$$\mathrm{s} = z_1 + \lambda \int z_1 dt \quad (23)$$

where λ is appositive constant.

Deriving from the above formula is:

$$\begin{aligned} \dot{\mathrm{s}} &= \dot{z}_1 + \lambda z_1 \\ &= f_1 \cdot x_2 - a_2 \cdot x_1 - d_1 - \dot{x}_{1\mathrm{d}} + \lambda \cdot (x_1 - x_{1d}) \end{aligned} \quad (24)$$

The expected displacement of the hydraulic cylinder which is designed to control the swing angle of the motor is x_{2d}, and then the expression of displacement tracking error of hydraulic cylinder is:

$$z_2 = x_2 - x_{2d} \quad (25)$$

Then the differential expression of the integral sliding surface is:

$$\begin{aligned} \dot{\mathrm{s}} &= f_1 \cdot z_2 + f_1 \cdot x_{2d} - a_2 \cdot x_1 \\ &\quad - d_1 - \dot{x}_{1\mathrm{d}} + \lambda \cdot (x_1 - x_{1d}) \end{aligned} \quad (26)$$

Substitute formula (17) into formula (26) to calculate, and we can get:

$$\begin{aligned} \dot{\mathrm{s}} &= \tilde{f}_1 \cdot z_2 + \hat{f}_1 \cdot z_2 + \tilde{f}_1 \cdot x_{2d} + \hat{f}_1 \cdot x_{2d} \\ &\quad - \tilde{a}_2 \cdot x_1 - \hat{a}_2 \cdot x_1 - \tilde{d}_1 - \hat{d}_1 \\ &\quad - \dot{x}_{1\mathrm{d}} + \lambda \cdot (x_1 - x_{1d}) \end{aligned} \quad (27)$$

Then the expression x_{2d} of the expected displacement of the hydraulic cylinder controlling the motor swing angle is:

$$x_{2d} = \frac{1}{\hat{f}_1} \begin{bmatrix} \hat{a}_2 \cdot x_1 + \hat{d} + \dot{x}_{1\mathrm{d}} - \lambda \cdot (x_1 - x_{1d}) \\ -k_1 s - k_2 \cdot \mathrm{sat}(s) \end{bmatrix} \quad (28)$$

where sat(s) is the saturated function, its expression is:

$$\mathrm{sat}(s) = \begin{cases} 1 & s > \Phi \\ \dfrac{s}{\Phi} & |s| < \Phi \\ -1 & s < -\Phi \end{cases}$$

In formula: Φ is the boundary layer and $\Phi > 0$.

Then substituting equation (28) into (27) can get: $\dot{\mathrm{s}} = \tilde{f}_1 \cdot x_2 - \tilde{a}_2 \cdot x_1 - \tilde{d}_1 - k_1 s - k_2 \cdot \mathrm{sat}(s) + \hat{f}_1 \cdot z_2$

Define Lyapunov function:

$$V_2 = V_1 + \frac{1}{2} k_{21} s^2 \quad (29)$$

The differentiation of the above formula is obtained as follow:

$$\begin{aligned} \dot{V}_2 &= \dot{V}_1 + k_{21} s \cdot \dot{s} \\ &= -k_{11} \tilde{x}_{1p}^2 \cdot \Gamma + \tilde{f}_1 (k_{11} \tilde{x}_{1p} \cdot x_2 + k_{14} \cdot \dot{\tilde{f}}_1) \\ &\quad + \tilde{a}_2 (k_{12} \cdot \dot{\tilde{a}}_2 - k_{11} \tilde{x}_{1p} \cdot x_1) + \tilde{d}_1 (k_{13} \cdot \dot{\tilde{d}}_1 - k_{11} \tilde{x}_{1p}) \\ &\quad + k_{21} s \cdot \left[\tilde{f}_1 \cdot x_2 - \tilde{a}_2 \cdot x_1 - \tilde{d}_1 - k_1 s - k_2 \cdot \mathrm{sat}(s) + \hat{f}_1 \cdot z_2 \right] \end{aligned} \quad (30)$$

The adaptive rate of the above formula is:

$$\begin{cases} \dot{\hat{f}}_1 = \dfrac{k_{11} \cdot \tilde{x}_{1p} x_2 + k_{21} \cdot s \cdot x_2}{k_{14}} \\ \dot{\hat{a}}_2 = -\dfrac{k_{11} \cdot \tilde{x}_{1p} x_1 + k_{21} \cdot s \cdot x_1}{k_{12}} \\ \dot{\hat{d}}_1 = -\dfrac{k_{11} \cdot \tilde{x}_{1p} + k_{21} s \cdot \tilde{d}_1}{k_{13}} \end{cases} \quad (31)$$

Then:

$$\begin{aligned} \dot{V}_2 &= \dot{V}_1 + k_{21} s \cdot \dot{s} \\ &= -k_{11} \tilde{x}_{1p}^2 \cdot \Gamma - k_3 s^2 \\ &\quad - k_4 s \cdot \mathrm{sat}(s) + k_{21} s \cdot \hat{f}_1 \cdot z_2 \end{aligned} \quad (32)$$

C. THE SPEED ADAPTIVE SOLUTION OF THE HYDRAULIC CYLINDER CONTROLLING THE SWING ANGLE

From $z_2 = x_2 - x_{2d}$ we can get:

$$\dot{z}_2 = \dot{x}_2 - \dot{x}_{2d} = x_3 - \dot{x}_{2d} \quad (33)$$

The expected speed of the hydraulic cylinder which is designed to control the swing angle of the motor is x_{3d}, then the expression of displacement tracking error of hydraulic cylinder is:

$$z_3 = x_3 - x_{3d}$$

Then:

$$\dot{z}_2 = z_3 + x_{3d} - \dot{x}_{2d} \quad (34)$$

Then the expression x_{3d} of the desired value of the speed of hydraulic cylinder controlling the motor swing angle is:

$$x_{3d} = \dot{x}_{2d} - k_5 z_2 - k_{21} s \cdot \hat{f}_1 \tag{35}$$

Then:

$$\dot{z}_2 = -k_5 z_2 - k_{21} s \cdot \hat{f}_1 + z_3 \tag{36}$$

Define Lyapunov function:

$$\mathrm{V}_3 = \mathrm{V}_2 + \frac{1}{2} z_2^2 \tag{37}$$

The differentiation of the above formula is obtained as follows:

$$\begin{aligned} \dot{\mathrm{V}}_3 &= \dot{\mathrm{V}}_2 + z_2 \cdot \dot{z}_2 \\ &= -k_{11} \tilde{x}_{1\mathrm{p}}^2 \cdot \Gamma - k_3 s^2 - k_4 s \cdot \mathrm{sat}(s) \\ &\quad + k_{21} s \cdot \hat{f}_1 \cdot z_2 + z_2 \cdot (-k_5 z_2 - k_{21} s \cdot \hat{f}_1 + z_3) \\ &= -k_{11} \tilde{x}_{1\mathrm{p}}^2 \cdot \Gamma - k_3 s^2 - k_4 s \cdot \mathrm{sat}(s) - k_5 z_2^2 + z_2 \cdot z_3 \end{aligned} \tag{38}$$

The expression of the integral sliding surface for the speed tracking error of the designed hydraulic cylinder is:

$$\mathrm{s}_2 = z_3 + \lambda_3 \int z_3 dt \tag{39}$$

The derivation of the above formula is as follows:

$$\begin{aligned} \dot{s}_2 &= \dot{z}_3 + \lambda_3 \cdot z_3 \\ &= \dot{x}_3 - \dot{x}_{3d} + \lambda_3 \cdot (x_3 - x_{3d}) \\ &= b_1 \cdot x_4 - b_2 \cdot x_3 - d_2 - \dot{x}_{3d} + \lambda_3 \cdot (x_3 - x_{3d}) \end{aligned} \tag{40}$$

If the expected value of the design servo valve outlet pressure is x_{4d}, the tracking error expression of the servo valve outlet pressure is:

$$z_4 = x_4 - x_{4d} \tag{41}$$

Collate:

$$\begin{aligned} \dot{s}_2 &= b_1 \cdot x_4 - b_2 \cdot x_3 \\ &\quad - d_2 - \dot{x}_{3d} + \lambda_3 \cdot (x_3 - x_{3d}) \\ &= b_1 \cdot (z_4 + x_{4d}) - b_2 \cdot x_3 - d_2 \\ &\quad - \dot{x}_{3d} + \lambda_3 \cdot (x_3 - x_{3d}) \end{aligned} \tag{42}$$

Define the state estimates of b_1, b_2, d_2 are $\hat{b}_1, \hat{b}_2, \hat{d}_2$, then the error of the state estimation can be expressed as follows:

$$\begin{cases} \tilde{b}_1 = b_1 - \hat{b}_1 \\ \tilde{b}_2 = b_2 - \hat{b}_2 \\ \tilde{d}_2 = d_2 - \hat{d}_2 \end{cases} \tag{43}$$

Then:

$$\begin{aligned} \dot{\mathrm{s}}_2 &= b_1 \cdot (z_4 + x_{4d}) - b_2 \cdot x_3 - d_2 - \dot{x}_{3d} + \lambda_3 \cdot (x_3 - x_{3d}) \\ &= \tilde{b}_1 \cdot z_4 + \tilde{b}_1 \cdot x_{4d} + \hat{b}_1 \cdot z_4 + \hat{b}_1 \cdot x_{4d} - \hat{b}_2 \cdot x_3 - \tilde{b}_2 \cdot x_3 \\ &\quad - \tilde{d}_2 - \hat{d}_2 - \dot{x}_{3d} + \lambda_3 \cdot (x_3 - x_{3d}) \end{aligned}$$

Then the expected value of servo valve outlet pressure x_{5d} can be expressed as:

$$x_{4d} = \frac{1}{\hat{b}_1} \begin{bmatrix} \hat{b}_2 \cdot x_3 + \hat{d}_2 + \dot{x}_{3d} - \lambda_3 \cdot (x_3 - x_{3d}) \\ -\dfrac{1}{k_{31} \cdot s_2} \cdot z_2 z_3 - c_3 \cdot s_2 \end{bmatrix} \tag{44}$$

After calculating we can get:

$$\dot{\mathrm{s}}_2 = \tilde{b}_1 \cdot x_4 + \hat{b}_1 \cdot z_4 - \tilde{b}_2 \cdot x_3 - \tilde{d}_2 - \frac{1}{k_{31} \cdot s_2} \cdot z_2 z_3 - c_3 \cdot s_2 \tag{45}$$

Define Lyapunov function:

$$\mathrm{V}_4 = \mathrm{V}_3 + \frac{1}{2} k_{31} s_2^2 + \frac{1}{2} \tilde{b}_1^2 + \frac{1}{2} \tilde{b}_2^2 + \frac{1}{2} \tilde{d}_2^2 \tag{46}$$

The differentiation of the above formula is obtained as follows:

$$\begin{aligned} \dot{\mathrm{V}}_4 &= \dot{\mathrm{V}}_3 + k_{31} s_2 \cdot \dot{s}_2 + \tilde{b}_1 \cdot \dot{\tilde{b}}_1 + \tilde{b}_2 \cdot \dot{\tilde{b}}_2 \\ &\quad + \tilde{d}_1 \cdot \dot{\tilde{d}}_1 - k_{11} \tilde{x}_{1\mathrm{p}}^2 \cdot \Gamma - k_3 s^2 - k_5 z_2^2 \\ &\quad + z_2 \cdot z_3 - k_4 s \cdot \mathrm{sat}(s) + \tilde{b}_1 \cdot \dot{\tilde{b}}_1 + \tilde{b}_2 \cdot \dot{\tilde{b}}_2 \\ &\quad + \tilde{d}_1 \cdot \dot{\tilde{d}}_1 + k_{31} s_2 \cdot (\tilde{b}_1 \cdot x_4 + \hat{b}_1 \cdot z_4 - \tilde{b}_2 \cdot x_3 \\ &\quad - \tilde{d}_2 - \frac{1}{k_{31} \cdot s_2} \cdot z_2 z_3 - c_3 \cdot s_2) \end{aligned} \tag{47}$$

Collate:

$$\begin{aligned} \dot{\mathrm{V}}_4 &= -k_{11} \tilde{x}_{1\mathrm{p}}^2 \cdot \Gamma - k_3 s^2 - k_4 s \cdot \mathrm{sat}(s) - k_5 z_2^2 \\ &\quad + k_{31} s_2 \cdot (\tilde{b}_1 \cdot x_4 + \hat{b}_1 \cdot z_4 - \tilde{b}_2 \cdot x_3 - \tilde{d}_2 - c_3 \cdot s_2) \\ &\quad + \tilde{b}_1 \cdot \dot{\tilde{b}}_1 + \tilde{b}_2 \cdot \dot{\tilde{b}}_2 + \tilde{d}_1 \cdot \dot{\tilde{d}}_1 \end{aligned}$$

The adaptive rate of the above formula is:

$$\begin{cases} \dot{\hat{b}}_1 = k_{31} s_2 \cdot x_4 \\ \dot{\hat{b}}_2 = k_{31} s_2 \cdot x_3 \\ \dot{\hat{d}}_2 = k_{31} s_2 \end{cases} \tag{48}$$

Then:

$$\begin{aligned} \dot{\mathrm{V}}_4 &= -k_{11} \tilde{x}_{1\mathrm{p}}^2 \cdot \Gamma - k_3 s^2 - k_4 s \cdot \mathrm{sat}(s) - k_5 z_2^2 \\ &\quad - k_{31} \cdot c_3 \cdot s_2^2 + k_{31} \cdot s_2 \cdot \hat{b}_1 \cdot z_4 \end{aligned} \tag{49}$$

where: k_3, k_4, k_5, k_{31} are the positive constants.

D. SOULATION OF CONTROL INPUT

Differential calculation of the tracking error expression $z_4 = x_4 - x_{4d}$ of the servo valve outlet pressure can be get:

$$\begin{aligned} \dot{z}_4 &= \dot{x}_4 - \dot{x}_{4d} \\ &= \mu \cdot g(x_4) - c_1 \cdot x_3 - c_2 \cdot x_4 - \dot{x}_{4d} \end{aligned} \tag{50}$$

where $g(x_4)$ is the expression of related to x_4.

Define Lyapunov function:

$$\mathrm{V}_5 = \mathrm{V}_4 + \frac{1}{2} z_4^2 \tag{51}$$

The derivation of the above formula is as follows:

$$\dot{\mathrm{V}}_5 = \dot{\mathrm{V}}_4 + z_4 \cdot \dot{z}_4$$

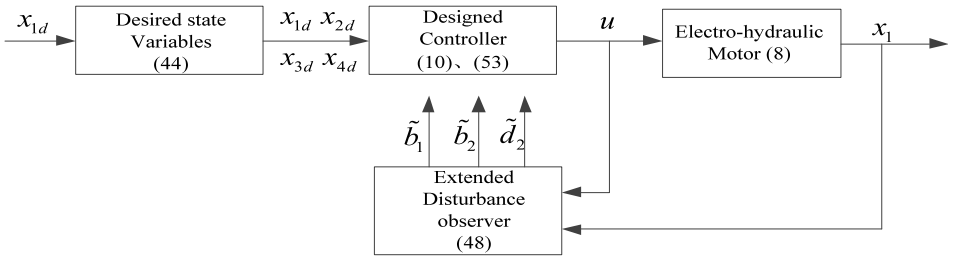

FIGURE 4. Figure Block diagram of the controller structure.

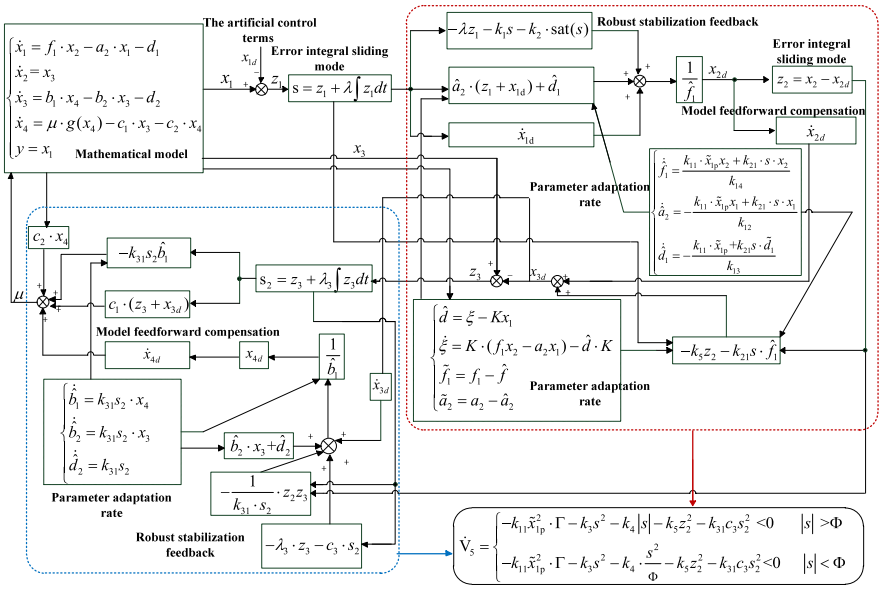

FIGURE 5. Motor speed control strategy based on back-stepping and adaptive state observer.

$$= -k_{11}\tilde{x}_{1p}^2 \cdot \Gamma - k_3 s^2 - k_4 s \cdot \mathrm{sat}(s) - k_5 z_2^2 - k_{31} c_3 s_2^2 + k_{31} s_2 \hat{b}_1 z_4 + z_4 \cdot [\mu \cdot g(x_4) - c_1 \cdot x_3 - c_2 \cdot x_4 - \dot{x}_{4d}] \quad (52)$$

The control input expression μ is designed:

$$\mu = \frac{1}{g(x_4)}(c_1 \cdot x_3 + c_2 \cdot x_4 + \dot{x}_{4d} - k_{31} s_2 \hat{b}_1) \quad (53)$$

Then substituting equation (53) into (52) can get:

$$\dot{V}_5 = \begin{cases} -k_{11}\tilde{x}_{1p}^2 \cdot \Gamma - k_3 s^2 - k_4 |s| - k_5 z_2^2 - k_{31} c_3 s_2^2 < 0 \\ \qquad |s| > \Phi \\ -k_{11}\tilde{x}_{1p}^2 \cdot \Gamma - k_3 s^2 - k_4 \cdot \dfrac{s^2}{\Phi} - k_5 z_2^2 - k_{31} c_3 s_2^2 < 0 \\ \qquad |s| < \Phi \end{cases} \quad (54)$$

From the above formula: $\dot{V}_5 < 0$, the design of the control system is stable and bounded. The design principle of the block diagram of the controller structure is shown in Fig. 4, and the whole control strategy design principle is shown in Fig. 5.

V. ANALYSIS OF EXPERIMENTAL RESULTS

A. DEVICE COMPOSITION

In order to study the proposed motor speed control strategy the land experiment bench has been built. As is shown in Fig. 6, the experimental platform is mainly consists of the test bench bracket, the hydraulic transmission system and the electric power processing system. The float is pulled up and down along the buoy by hoists which are employed to simulate the float motion under different wave conditions, the hydraulic cylinder moves simultaneously with the float motion. It can convert mechanical energy into hydraulic energy.

The hydraulic transmission system is shown in Fig. 7. The output parameters of hydraulic transmission system and power processing system can be real-time collected through the upper computer. The collected parameters are fed back to the host computer through Ethernet. The software Matlab and AMEsim are used to establish control strategy in the host computer. The posed motor speed control strategy is obtained by using equations (1)-(54), while the reference controller was designed based on the proportional integral derivative (PID) algorithm.

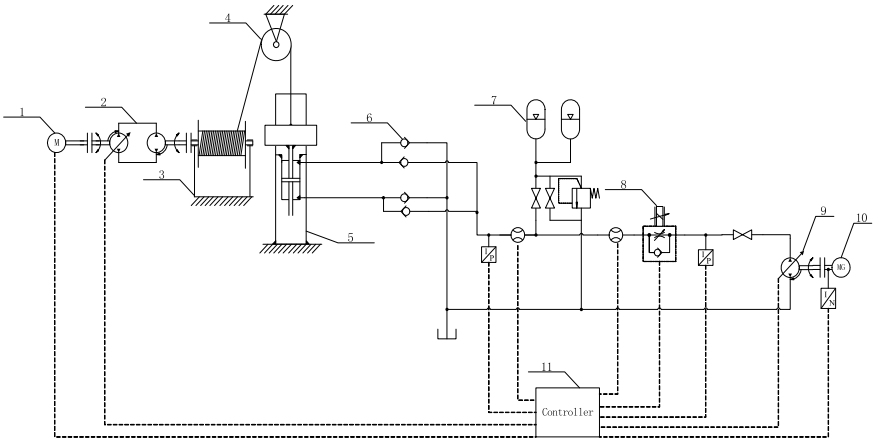

1.Electric motor 2. Combination design of the pumps 3. Windlass 4. Pulley systems 5.Buoy 6. Check valve 7.Accumulator 8. Electro-hydraulic proportional control valve 9. Variable displacement motor 10. Electric generator 11. Controller

FIGURE 6. Schematic diagram of the land experimental platform.

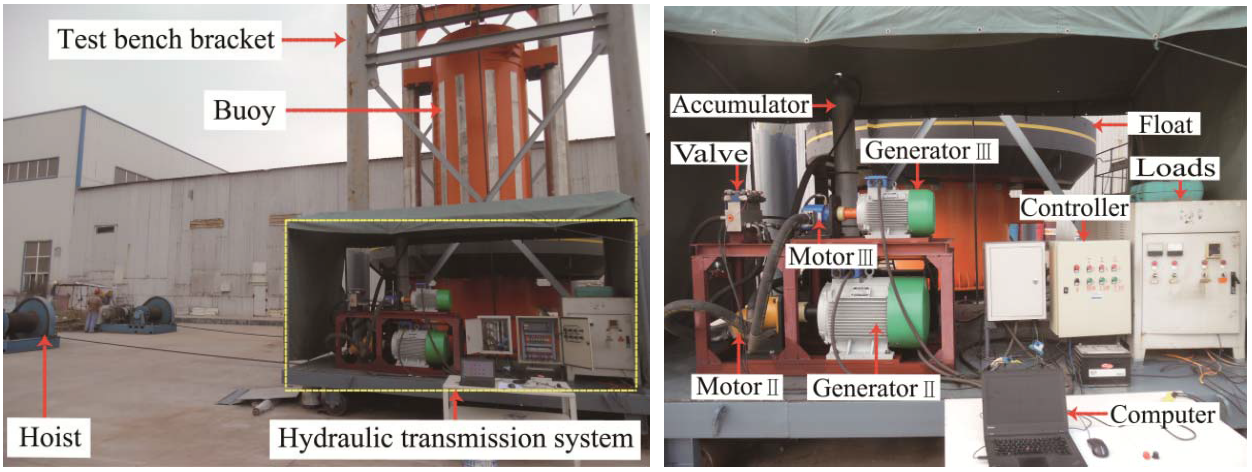

FIGURE 7. Experimental apparatus and hydraulic transmission system.

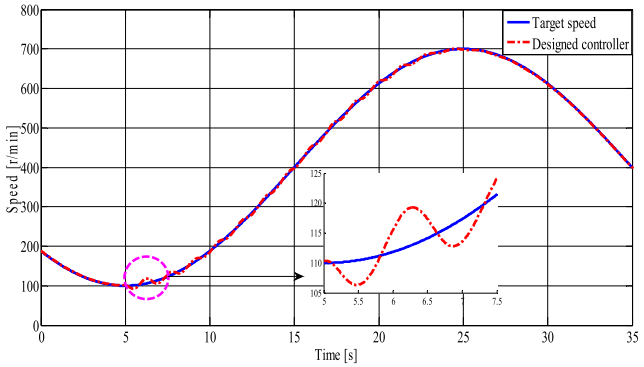

FIGURE 8. Speed control curves of hydraulic motor.

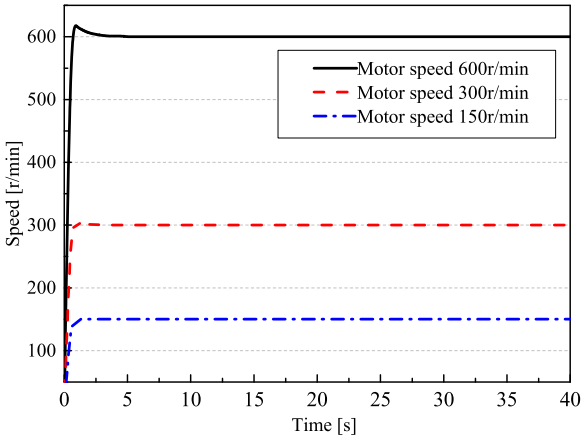

FIGURE 9. Response curves of different constant speed control.

B. MOTOR SPEED TRACKING RESPONSE ANALYSIS UNDER SINE SIGNAL REQUIREMENT

Set the load torque to 50 Nm, the working state of control strategy under sinusoidal velocity tracking is analyzed. Fig. 8 shows the speed tracking speed curve of the hydraulic motor. By analyzing the curves, it can be concluded that the maximum error of motor speed is 5 r/min when the load disturbance is added at 5s, and the speed tracking produces oscillation. After two seconds the disturbance is overcome and the speed error is reduced, thus the motor speed is

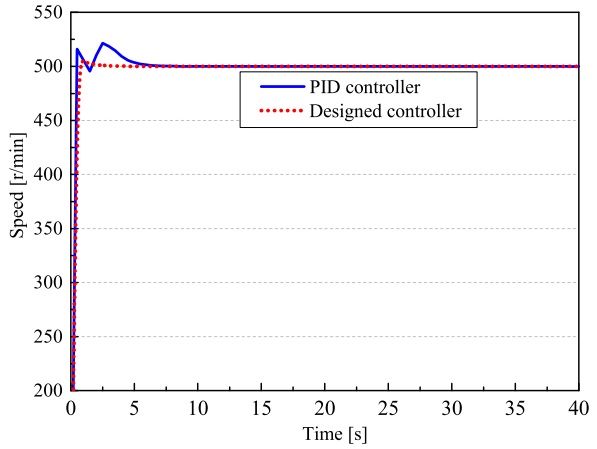

FIGURE 10. Constant speed control curves of hydraulic motor.

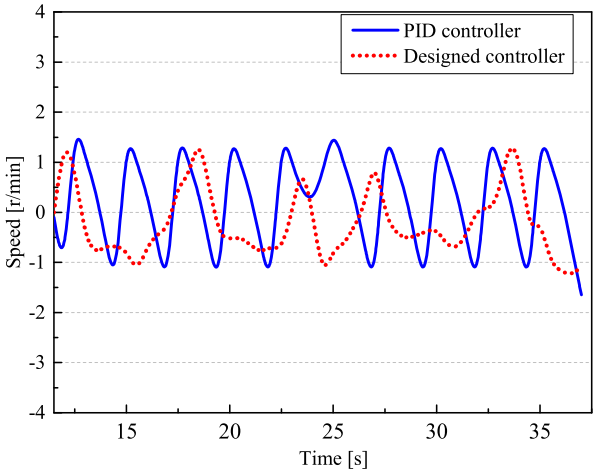

FIGURE 11. Constant speed control error curves of hydraulic motor.

restored to the tracking target speed. The designed controller can resist external interference to satisfy ocean engineering needs.

C. MOTOR SPEED TRACKING RESPONSE ANALYSIS UNDER CONSTANT NUMERICAL REQUIREMENT

Set the load torque to 50 Nm and the expected speed of the motor is 600 r/min, 300 r/min and 150 r/min respectively. Study the response state of motor speed control under different set speeds. The results are shown in Fig. 9.

Analysis of the curve in Fig. 9 can get that the designed control algorithm can be used to realize the desired speed control of the motor, the regulation characteristics are basically the same under different set speeds, but the higher the expected value of speed regulation is, the larger the overshoot is, and the setting of initial target speed will affect the control accuracy.

Fig. 10 shows the response curve of PID control strategy and designed control strategy when the targeted speed is 500r/min, Fig. 11 shows the speed error curve.

By analyzing the motor speed curve and error curve it can be concluded that compared with PID control strategy, the overshoot of hydraulic motor is obviously smaller under

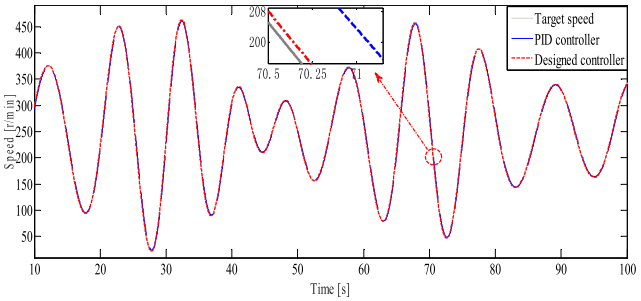

FIGURE 12. Irregular speed requirement curves of motor.

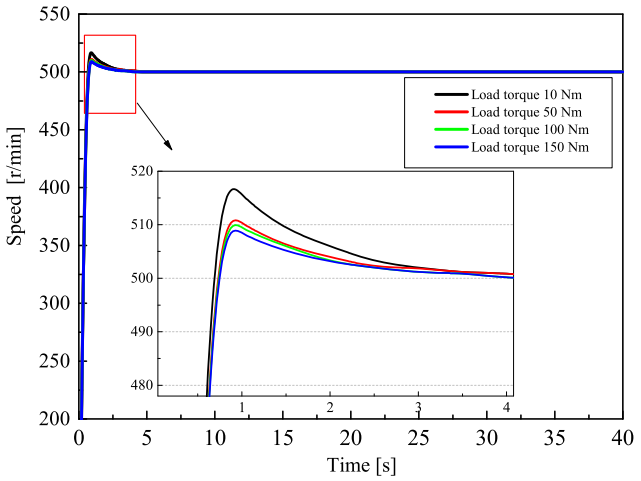

FIGURE 13. Output curves of speed control under different loads.

the designed controller, the regulation time is about 0.5s, the error range is 0.2% of the target speed. The designed control strategy can adjust the motor swing angle in time according to the input speed require and can achieve the speed tracking to the targeted more accurate.

D. MOTOR SPEED TRACKING RESPONSE ANALYSIS UNDER IRREGULAR SIGNAL REQUIREMENT

Considering the characteristics of waves, the working state of the control strategy is analyzed. Set the load torque to 50 Nm and the expected speed of the motor is irregular signal. Then analyze the response state of motor speed control. The curves are shown in Fig. 12. By analyzing the curves we can get: Under the condition of irregular speed tracking, the designed control strategy can also achieve the target speed tracking control, but because the curve data range is large, the curve fluctuation is not obvious. After amplifying the curve, it can be seen that the speed error of PID controller is about 4%, and that of the designed controller is about 1.2%. After considering the characteristics of the wave, the rotational speed error increases, but it can still meet the design requirements.

E. HYDRAULIC MOTOR SPEED REGULATION UNDER DIFFERENT LOAD TORQUE

The change of the load torque will affect the pressure of the system, cause the system pressure to fluctuate greatly or

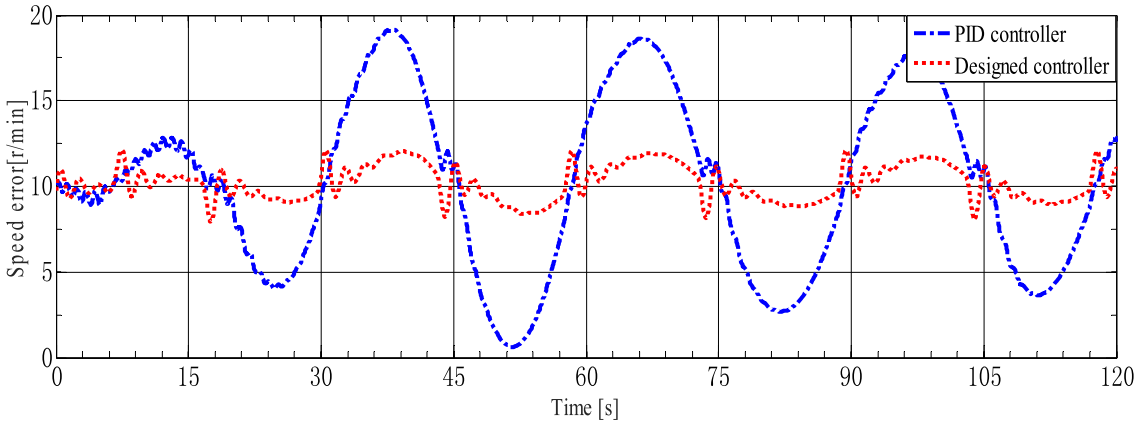

FIGURE 14. Output curves of speed control under 150 Nm loads.

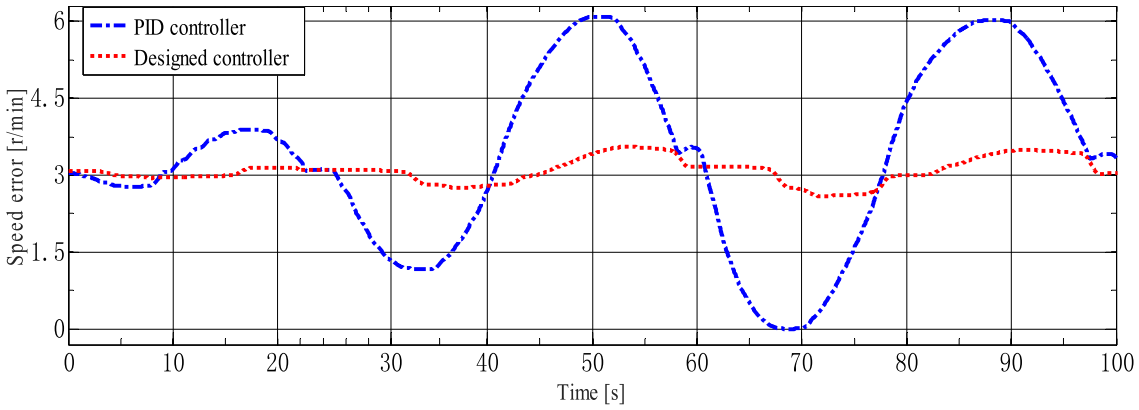

FIGURE 15. Output curve of speed control under 50 Nm loads.

slightly, If the flow required by the system cannot be provided in time, the pressure will drop; otherwise, if the system only needs less flow and the redundant flow cannot be released in time, the pressure will rise. By controlling the displacement of the variable motor, the flow and torque of system can be adjusted indirectly, so that the speed of the motor can maintain different stable values in the different stage range.

When the test speed is inconsistent with the set speed, the speed difference can drive the proportional valve to work through the controller. The output flow of the proportional valve controls the movement of the hydraulic cylinder of the variable displacement motor. The movement of the hydraulic cylinder adjusts the swash-plate angle of the hydraulic motor, so as to change the displacement of the motor, make the output torque consistent with the load torque, and finally make the output speed reach the set value.

For example, when the load torque increases, assuming that the output torque is less than the load torque, the speed of variable motor will inevitably decrease. At this time, the measured speed is less than the set speed, and the speed difference will go through the controller to increase the displacement of the hydraulic cylinder, thus to increase the motor displacement and the output torque. Finally, the drive torque and load torque are consistent, and the speed is restored to the set value so as to achieve the goal of outputting stable speed.

The torque balance equation of variable motor is as follows:

$$Vm = \frac{Qm \cdot \eta m}{nm} \tag{55}$$

$$Tm = Jm \cdot \dot{\omega} m + Mm = Vm \cdot PL - B \cdot \omega m \tag{56}$$

In formula:

Vm is the displacement of motor; Qm is the flow of motor; nm is the speed of motor; ηm is the volume efficiency of motor; Tm is the output torque for motor;Jm is the motor output moment of inertia;ωm is the motor output speed;M_m is the motor load torque;Vm is the output displacement for motor;P_L is the load differential pressure;B is the viscous damping coefficient of the load.

Fig. 13 are the motor speed tracking response curves under the designed controller, when the target speed of the motor is 500r/min, and the load torque are:10Nm, 50Nm, 100Nm, 150Nm respectively.

By analyzing the above curves, we can get: when the external load is 10Nm, the system regulation time is 0.3s, the overshoot is 0.4%; when the load is 50Nm, the system regulation time is 0.32s, the overshoot is 0.36%; when the external load is100Nm, the system regulation time is 0.35s, the overshoot is 0.33%; when the load is 150Nm, the system regulation time is 0.40s, the overshoot is 0.29%. The

results show that with the increase of the external load torque, the speed regulation response of the system slows down, the overshoot decreases, and the stable output performance is basically unchanged. It shows that the designed control algorithm can effectively ensure the motor speed within the expected range. Considering the characteristics of waves, the output curves of speed control under 50 Nm loads and 150 Nm loads are shown in Fig. 14 and Fig. 15.

Analyze Fig. 14 and Fig. 15 we can get that, when the load is different, there are different speed output errors. When the load is 150Nm, the speed error under the PID control strategy is 20r/min, the maximum speed error under the designed controller is 10r/min, and when the load is 50Nm, the speed error under the PID control strategy is 6r/min and the speed error under the designed controller is 4r/min. Compared with PID control algorithm, the designed controller has smaller error and can achieve better speed control requirements. The results also show that when the load is small, it is easier to achieve accurate control.

VI. CONCLUSION

A variable-displacement motor speed controlled strategy has been presented to smooth the motor speed, design details and dynamic modeling of the controlled strategy have been presented. The state equation of variable motor volume speed regulation is established. In the process of building the back-stepping control method, the method based on Lyapunov stability criterion is used to design the adaptive parameters so as to approach unknown interference. At the same time, in order to eliminate the approach error of the adaptive system, the integral sliding mode theory is used to compensate it. During this process the nonlinear control strategy is designed and the control input u is solved. The control strategy can overcome the oscillation of motor speed and improve the stability of power output when load disturbance occurs. Comparative experimental results have demonstrated that the proposed controller have better performance of stable output speed compared with the conventional PID controller under different speed tracking requirements. The method also improved the stability of motor volume speed regulation under different external loads.

REFERENCES

[1] Y. Lin, J. Bao, H. Liu, W. Li, L. Tu, and D. Zhang, "Review of hydraulic transmission technologies for wave power generation. Review of hydraulic transmission technologies for wave power generation," *Renew. Sustain. Energy Rev.*, vol. 50, no. 2, pp. 194–203, 2015.

[2] S. Kosai, "Dynamic vulnerability in standalone hybrid renewable energy system," *Energy Convers. Manage.*, vol. 180, pp. 258–268, Jan. 2019.

[3] J. F. Gaspar, M. Calvário, M. Kamarlouei, and C. G. Soares, "Design tradeoffs of an oil-hydraulic power take-off for wave energy converters," *Renew. Energy*, vol. 129, pp. 245–259, Dec. 2018.

[4] T. D. Dang, M. T. Nguyen, C. B. Phan, and K. K. Ahn, "Development of a wave energy converter with mechanical power take-off via supplementary inertia control," *Int. J. Precis. Eng. Manuf.-Green Technol.*, vol. 6, no. 3, pp. 497–509, Jul. 2019.

[5] A. Babarit, J. Singh, C. Mélis, A. Wattez, and P. Jean, "A linear numerical model for analysing the hydroelastic response of a flexible electroactive wave energy converter," *J. Fluids Struct.*, vol. 74, pp. 356–384, Oct. 2017.

[6] H. Gao and Y. Yu, "The dynamics and power absorption of cone-cylinder wave energy converters with three degree of freedom in irregular waves," *Energy*, vol. 143, pp. 833–845, Jan. 2018.

[7] X.-Y. Yang, H.-S. Zhang, and H.-T. Li, "Wave radiation and diffraction by a floating rectangular structure with an opening at its bottom in oblique seas," *J. Hydrodyn.*, vol. 29, no. 6, pp. 1054–1066, Dec. 2017.

[8] Y.-J. Wang and C.-K. Lee, "Dynamics and power generation of wave energy converters mimicking biaxial hula-hoop motion for mooring-less buoys," *Energy*, vol. 183, pp. 547–560, Sep. 2019.

[9] Y. M. Shen, Y. H. Zheng, and Y. G. You, "On the radiation and diffraction of linear water waves by a rectangular structure over a sill," *Infinite Domain Finite water depth. Ocean Eng.*, vol. 32, no. 9, pp. 1073–1097, 2005.

[10] J. H. Todalshaug, G. S. Ásgeirsson, E. Hjálmarsson, J. Maillet, P. Möller, P. Pires, M. Guérinel, and M. Lopes, "Tank testing of an inherently phase-controlled wave energy converter," *Int. J. Mar. Energy*, vol. 15, pp. 68–84, Sep. 2016.

[11] Y. Cen and Z. Yongliang, "Experimental study on operation characteristics of wave energy pressure pump," *J. Water Conservancy*, vol. 12, no. 9, pp. 1107–1111, 2013.

[12] Z. Wei, Z. XiaoRong, Z. Jianchao, "Reactive power and voltage coordinated control research of wind farm adopting doubly-fed induction generators," *Adv. Mater. Res.*, vol. 1003, pp. 152–155, 2014.

[13] J. F. Gaspar, M. Calvário, M. Kamarlouei, and C. Guedes Soares, "Power take-off concept for wave energy converters based on oil-hydraulic transformer units," *Renew. Energy*, vol. 86, pp. 1232–1246, Feb. 2016.

[14] H. Shi, F. Cao, Z. Liu, and N. Qu, "Theoretical study on the power take-off estimation of heaving buoy wave energy converter," *Renew. Energy*, vol. 86, pp. 441–448, Feb. 2016.

[15] Y.-C. Chow, Y.-C. Chang, D.-W. Chen, C.-C. Lin, and S.-Y. Tzang, "Parametric design methodology for maximizing energy capture of a bottom-hinged flap-type WEC with medium wave resources," *Renew. Energy*, vol. 126, pp. 605–616, Oct. 2018.

[16] V. Rayamajhee and A. Joshi, "Economic trade-offs between hydroelectricity production and environmental externalities: A case for local externality mitigation fund," *Renew. Energy*, vol. 129, pp. 237–244, Dec. 2018.

WEI ZHANG received the Ph.D. degree in electrical engineering from Shandong University, Jinan, China, in 2018. He is currently a Lecturer with the Institute of Marine Science and Technology, Shandong Jianzhu University, Jinan. His research interests include the operation and planning of the power systems, the influence of new energy to the power systems, and the stability and reliability of the wave power systems.

SHIZHEN LI (Member, IEEE) received the Ph.D. degree in fluid power transmission and control from Zhejiang University, Hangzhou, China, in 2016. He is currently a Lecturer with the Institute of Marine Science and Technology, Shandong University, Qingdao, China. His research interests include design, modeling, identification, nonlinear control of electro-hydraulic servo systems, and ocean engineering.

YANJUN LIU received the Ph.D. degree in electrical engineering from Shandong University, Jinan, China. He is currently a Lecturer with the Institute of Marine Science and Technology, Shandong University. His research interests include the operation and planning of the power systems and ocean engineering.